Study on AE characteristics of concrete with different w/c ratio under uniaxial compression

Aiping Yu [1], Zhehan Chen [1], Lu Zhang [1], Xiuxin Li [1], Jinxu Shi [1], Feng Fu [1, 2] * *

1. College of Civil and Architectural Engineering, Guilin University of Technology, Guilin 541004.

2. Department of Engineering, School of Science & Technology, City, University of London, Northampton Square, London, EC1V 0HB, U.K

Abstract: Concrete material is a three-phase composite material. Its acoustic emission (AE) characteristics are influenced by the properties of its components. The water-cement ratio has significant influence on the mechanical properties and components of concrete. To clarify the relationship between water-cement ratio and AE characteristics of concrete, in this study, AE characteristics of concrete with different water-cement ratio were discussed through parameter analysis and frequency domain analysis. A damage evaluation model of concrete was established based on AE events,cumulative AE ringing count (CR) and cumulative energy (CE).The results show that AE parameters can characterize the three-stage failure process of concrete, namely the initial stage, the stable stage and the active stage.The water-cement ratio has obvious influence on the damage process of concrete and the time distribution of AE parameters.With the development of the damage process, AE signals shift from 30 kHz to 300 kHz and higher frequencies, and the number of main frequency segments increases. On this basis, the evaluation model *D* of concrete compression damage based on the CR and CE was established. The tangent slope of *D* was used to observe the change of damage stage, which is in good agreement with the experimental results.

Keywords: Acoustic Emission (AE), water-to-cement ratio, microcrack, damage process, damage assessment

1. Introduction

Acoustic Emission(AE) refers to the phenomenon of an object or material rapidly releases energy and emits a transient elastic wave when deformation or crack expansion occurs by an external or internal force[1] . The elastic wave propagates throughout the structure, causing mechanical vibrations to occur on the surface of the structure, which are picked up by sensors mounted on the structure and generate an output voltage in terms of a detected AE signal. The AE characteristics are obtained after the signal is selected and processed by appropriate data analysis. AE parameters can provide the main information of material damage and fracture, and are the main indexes of material damage evaluation.

Concrete is a heterogeneous material consisting of three-phase component: aggregates, mortar and ITZ[2] . Refraction, diffraction, and energy attenuation occur when AE waves propagate inside the concrete material when they encounter discontinuous boundaries (pores, cracks, etc.) or aggregate interfaces, resulting in severe distortion of the waveform[3] . At this time, direct judgments of structural damage according to the signals received by AE instruments are prone to erroneous conclusions. Therefore,it is particularly important to consider the wave

* Corresponding author: E-mail address: feng.fu.1@city.ac.uk

propagation characteristics when monitoring material damage using AE techniques.

The essential premise of this study is that the AE response during damage to complex, heterogeneous[5] materials such as concrete is influenced by the development behavior of cracks, which depends on the properties of its components. Clarifying the effect of raw material composition ratio on the AE properties of concrete materials is the basis for effective damage monitoring of concrete structures using AE techniques, which is of great significance for damage monitoring of practical projects. Wu et al.[6] found that the fracture energy of concrete is related to the maximum particle size, and AE characteristic parameters can reflect the fracture energy of concrete. Chen et al.[7] found that concrete with different aggregate grain sizes have different crack tip fracture characteristics and fracture process zone (FPZ), which correspond well with AE parameters. Elapra et al.[8] concluded that sand rate has some degree of influence on cumulative AE events and localization results. Lee et al.[9] analyzed the variation of time and frequency domain parameters during compression damage of concrete with different sand contents. Wang et al.[10] used AE technology to reveal the failure mechanism of concrete microstructure, and AE characteristic parameters were successfully used to reflect the physical mechanism of concrete damage process. Ranjith et al.[12] analyzed the AE response of concrete with different water contents.They found that the water content changed the number of AE events during compression failure. Kocur et al.[13] verified the effect of aggregate particle size and pore space, etc. in concrete on AE wave propagation behavior. Li et al.[15] identified the relationship between acoustic emission characteristic parameters and concrete crack propagation rate. Fu et al.[16] confirmed that the aggregate grade of asphalt concrete has a significant influence on its acoustic emission characteristics. AE characteristic parameters can characterize the failure process of asphalt concrete.

The above studies show that the influence of concrete composition on AE wave propagation is a problem that cannot be ignored in AE damage monitoring, which has gradually attracted the attention of scholars[17] . However, unfortunately, such studies are still rare, and researchers usually choose the parameters they are interested in for testing and analysis according to the instruments they have, causing arbitrariness in the selection of parameters, thus making the test results lack of comparability.

The mechanical properties are strongly influenced by the pore structure,which is one of the most important properties of concrete[18] . Similarly, the pore structure also affects the propagation behavior of AE waves. This influence is mainly reflected in two aspects.

(1) Cement paste and aggregate have approximate acoustic impedance coefficient (10^7 kgs/m^3). However, the acoustic impedance coefficient of air filled in pores and cracks (1.3 kgs/m^3) is much smaller than that of the first two solid components. As shown in Fig. 1, AE waves cannot propagate directly through the air in pores and fractures, and reflections and bypasses occur at the pore and fracture interfaces, which complicate their propagation behavior.

(2) Literature[19] showed that there is a kind of larger pores existing in ITZ, compared to the cement mortar without coarse aggregates. With the increase of the w/c ratio, these larger pores in the ITZ also increase, which affects the AE wave propagation path. In addition, the strength of ITZ and paste play an crucial role in the fracture behavior of concrete. For concrete with relatively high w/c, the strength of ITZ and paste is relatively low due to the higher porosity, so most cracks occur in ITZ and paste[20] . It is found in literature [21] that ITZ has a significant influence on the compressive damage process of concrete through numerical simulation, and these simulation

results are further verified in the experiment. As the weakest phase in concrete, ITZ has significant porosity and low strength and stiffness[25] Therefore, ITZ is usually the starting point of concrete damage and dominates the load-bearing capacity of concrete and its failure mechanism, and the role of ITZ and paste in the damage process depends on the w/c ratio. Huang et al.[26] found that the microcrack initiation of concrete occurs mainly in the ITZ zone. At the same stress level, concrete with higher w/c ratio has more internal micro-cracks and wider crack system. In the paste with high w/c ratio, the effect of ITZ is more obvious at the beginning of crack extension, while in the paste with low w/c ratio, the effect of ITZ is especially important at the rapid crack extension. As the w/c ratio varies, ITZ has different effects on the concrete damage process, thus affecting the generation of AE phenomena and the propagation of AE waves. Kim et al.[27] investigated the relationship between w/c ratio and porosity, and the results showed that when the degree of hydration is certain, the increase of w/c ratio significantly increases the total porosity. Literature[28] the numerical simulation results show that high porosity concrete produces more cracks during the damage process of concrete with different ITZ porosity.

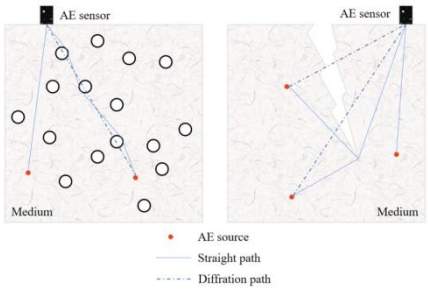

Fig.1 Effect of pore and crack on propagation path of AE elastic wave

In summary, the w/c ratio has a huge influence on the three-phase ratio of concrete and, in turn, on the evolution of cracks during damage. Theoretically, such an effect would lead to differences in the propagation characteristics of AE waves during damage in concrete with different w/c ratios, so the w/c ratio might be used as the main indicator parameters to characterize the effect of concrete raw material composition ratio on AE characteristics. Therefore, this paper studies the AE characteristics of concrete specimens with different w/c ratios under uniaxial compression.The damage stage of concrete is described by AE characteristic parameters. Since the existing methods (such as B-value method) rely on manually set thresholds and introduce errors that are difficult to eliminate, this paper proposes to use the change of AE frequency domain signal as the precursor of concrete fracture, and establishes a concrete damage evaluation model based on AE characteristic parameters to avoid the errors introduced by humans.Based on this, this paper mainly expounds the following four aspects of content:

(1) Equipment and procedures for AE monitoring and uniaxial compression test (Section 2).

(2) The relationship between damage mechanism of concrete and AE characteristic parameters and the influence of w/c ratio on them (Section 3.1 and Section 3.2).

(3) The relationship between damage mechanism of concrete and AE frequency domain characteristic (Section 3.4).

(4) The damage evaluation model of concrete based on AE characteristic (Section 4).

2. Experimental investigations

2.1.Material and mix design

Ordinary Portland cement, water, fine aggregate and coarse aggregate were used as the raw materials in this study.The ordinary Portland cement (PO42.5 cement) meets Chinese standards.Fine aggregate and coarse aggregate were all washed by water and dried.The coarse aggregate adopts the continuous gradation of 5-20 mm. Other related physical performance indexes of aggregate are shown in Table 1 .Concrete specimens with the w/c ratios of 0.58, 0.48 and 0.38 were prepared in this study, with six specimens in each group. The combination of specimens is shown in Table 2 . The proportion of sand to concrete was 0.35. The specimens were demolded after 24 h of casting and were then subjected to standard curing at a temperature of 20°C and a curing humidity of 95%.

Table 1 Physical performance indexes of aggregate

	Fineness modulus	Accumulated density（g/cm^3）	Accumulated density（g/cm^3）
Fine aggregate	2.83	2.63	1.53
Coarse aggregate	—	2.63	1.44

Table 2 The mix proportions of concrete

W/C ratio	Cement（kg/m^3）	Water（kg/m^3）	Sand（kg/m^3）	Macadam（kg/m^3）
0.58	458.72	266.06	534.05	991.80
0.48	500.3	240.1	545.6	1013.2
0.38	550.1	209.0	559.4	1038.8

2.2.Test program

AE parameter analysis is the most commonly used AE analysis method to explore the relationship between AE parameters and the evolution process of material damage. Therefore, uniaxial compression tests are conducted on specimens and simultaneous AE monitoring is performed during the compression tests.

2.2.1.Test setup

The test system is composed of loading facility and AE facility. The loading facility adopts 300 t pressure testing machine. The AE facility uses the PAC-3rd generation 16-channel fully digital system AE device.Sensors are PK15I narrow-band resonance sensor. The relevant test parameters are shown in Table 3. The test specimens are 3 groups of concrete cubes, and each group consists of six concrete specimens with dimensions of 150mm× 150mm× 150mm, and the same batch was poured and maintained. Figure 2 and Figure 4 show the test system and sensor layout.

Table 3 Test parameters of AE system

Parameter	Threshold（dB）	Floating Threshold（dB）	PDT（μs）	HDT（μs）	HLT（μs）	Sampling rate(MSPS)	Sampling length
Value	35	5	100	200	300	1	1000

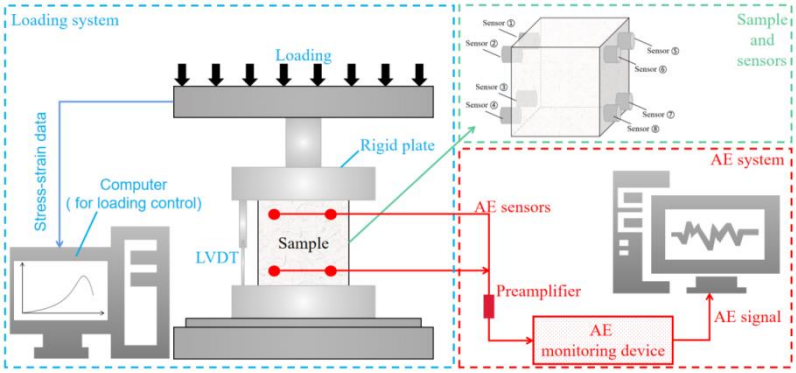

Fig.2 Schematic diagram of experimental setup

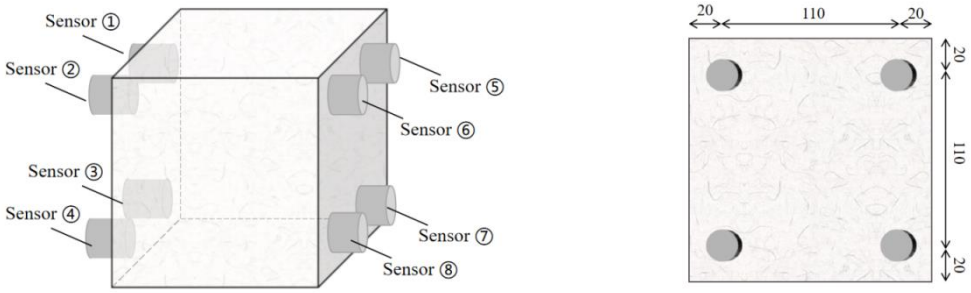

(a)Sensor numbers (b)Sensors layout

Fig.3 Sensors layout diagram of cube

2.2.2.Test procedures

To improve the signal quality, we polished the specimen surface before the experiment. Sensors were attached to the surface of the specimen using hot melt adhesive as coupling agent. After the sensors were installed, the AST function is used to check the coupling condition to ensure a good coupling between the sensor and the sample surface.

Uniaxial compression test is performed on concrete specimens at the loading rate of 0.1 MPa/s, and the stress-time diagram is automatically recorded. AE signals were recorded with AE equipment, and the AE test was started and terminated simultaneously with the loading test. To reduce the error during the test, the same test was performed on all samples.

3. Results and discussion

In this section, uniaxial compressive tests were conducted on concrete specimens with different w/c ratios to obtain the time-domain characteristics of AE parameters.To fully reflect the AE characteristics of the specimens, suitable AE parameters should be selected[29] . Currently, the parameters used by scholars to study AE time-domain characteristics are mainly AE event numbers[30] , AE hit count[31] , AE energy[32] , AE Ringing Count[33] and AE frequency[34] etc. Among them, the AE event count reflects the number of AE events in whole loading process, so this paper starts with the AE event count for analysis.

3.1.AE events

From the analysis of the stress-time curves and AE event number-time curves shown in Fig. 4, it is clear that the specimens with different w/c ratios undergo a similar three-stage process during the uniaxial compression history , i.e., the initial stage (OA), the stable stage (AB), and the unstable active stage (BC).

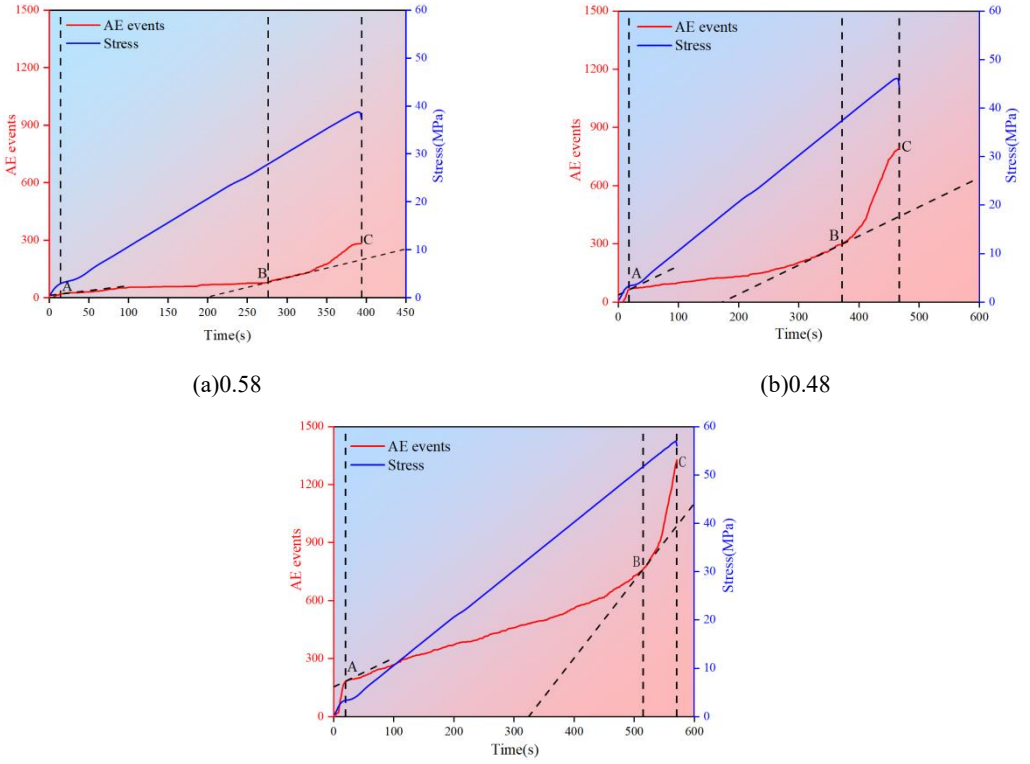

(a)0.58 (b)0.48

(c)0.38

Fig.4 Accumulative number of AE events, loading related to time

(1)During the OA stage, the concrete specimen starts to be loaded. Due to the small load value, the stress-strain curve basically changes in a straight line. At this time, the pores inside the concrete are compacted and the primary microcracks are closed by compression, which leads to the change of the internal microstructure of the concrete. The AE events in this stage mainly come from the compaction of pores or the closure of primary microcracks, so there are just a few AE events and AE event accumulation curve increases slightly. This stage accounts for about 5% to 10% of the whole AE process.

(2)In the AB stage, the cracks on the bond surface of mortar and aggregate are compressive-shear composite stresses. With the increasing load, the mortar and aggregate begin to slide along the crack surface. At this time, the primary microcrack reopens after the compressive closure in the OA stage, and the width continues to develop, driving the crack tip to expand into the mortar and increasing the crack length. At the same stage, the nascent microcrack starts cracking from the ITZ and gradually expands into the matrix to form a certain scale. This is a continuous and stable development process, and the AE event accumulation curve develops gently. This stage accounts for about 65% to 87% of the whole AE process.

(3)At the beginning of the BC stage, as it approaches, the ultimate load the cracks that continue to develop in the stable stage form an extensive and continuous fracture system, and the crack expansion enters the unstable expansion stage, where the matrix cracks expand rapidly and the deformation of the specimen increases, eventually leading to destabilization damage. At this stage, a great deal of AE events were collected, so the AE event accumulation curve becomes very steep with the significant increase of AE events. In BC stage, a distinct crack expansion process can be

observed along with cracking sound. This stage accounts for about 15% to 30% of the whole AE process.

By comparison, we found that as w/c ratio decreased, the proportion of AB phase gradually increased and AE events collected gradually increased, while the proportion of OA and BC phases gradually decreased.

(1)The smaller the w/c ratio, the denser the internal structure of the specimen, so the OA phase of the low w/c ratio specimen accounts for a smaller proportion of the whole AE process than that of the high w/c ratio specimen.

(2)The higher the w/c ratio of the specimens, the weaker the ITZ, the easier the cracks are produced, the faster they enter the BC stage, and the shorter the AB stage. The results show that: in the specimens with lower w/c ratio, the transition zone is narrower, but more microcracks are produced, so the number of AE events in AB stage is higher in the specimens with lower w/c ratio.

(3)In the BC stage, due to more microcracks and more serious stress concentration phenomenon, the low w/c ratio specimens will be rapidly destabilized and damaged, so the percentage of BC stage of low w/c ratio specimens is smaller.

The above laws indicate that the AE event counts have a strong relationship with the damage development process of the specimen under the load. In order to model the relationship between AE parameters and the damage development process, we also need to select the parameters that are most closely related to the damage development process for analysis. AE ringing counts can reflect the amplitude of the AE signal, thus showing the strain energy released during the damage process; AE energy is the area of the waveform envelope, which is very sensitive to the change of stress level. Therefore, these two parameters are selected for further analysis in this paper.

3.2.AE ringing counts and energy

Figure 5 shows the relationship between ringing counts and cumulative ringing counts (CR), energy and cumulative energy (CE) with the time course of uniaxial compression, respectively. From the overall curves, the CR and CE curves are similar to the AE event number curves in Fig. 4 throughout the uniaxial compression damage process, and the distributions of ringing count and energy correspond to the changes of CR and CE curves, respectively, so this section continues the three stage division of OA, AB and BC in Section 3.1. The following analysis is carried out as an example for the samples set with w/c ratio of 0.58.

At the beginning of the OA stage (around 0-1% of the peak stress), there is a difficult to detect period when both AE ringing counts and AE energy are low due to the loading rate. It is after this phase that the AE ringing counts and AE energy increases, because at the beginning of loading, the pores inside the concrete are not yet compacted and the primary microcracks are not yet closed by pressure, so the ringing counts and energies are low.

As the load increases, in the middle of the OA stage (about 1-8% of the peak stress), the pores inside the concrete are compacted, and at this time the AE events mainly come from the damage to the tiny units inside the concrete, which are more in number but not serious, so the AE ringing counts are higher and the AE energy is lower. At the same time, the primary cracks are also closed by compaction, and the contact between different interfaces inside the concrete becomes more and the friction becomes larger, which also leads to the increase of AE ringing counts.

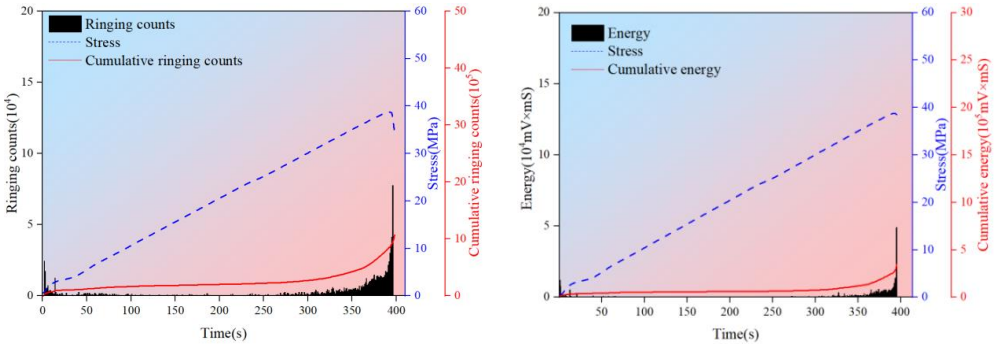

(a)0.58

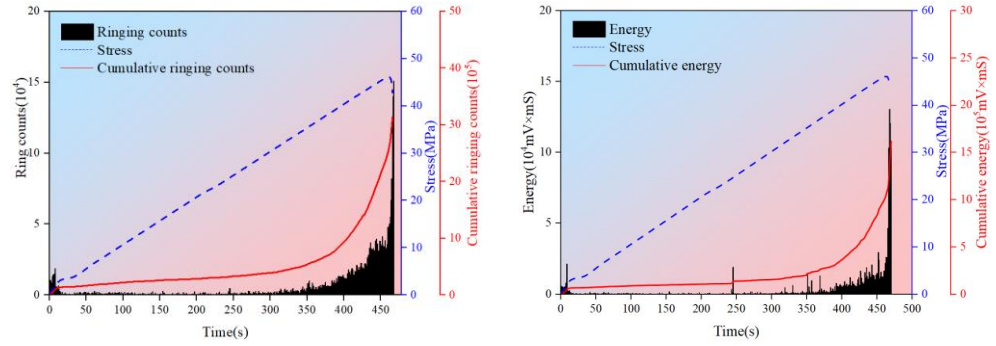

(b)0.48

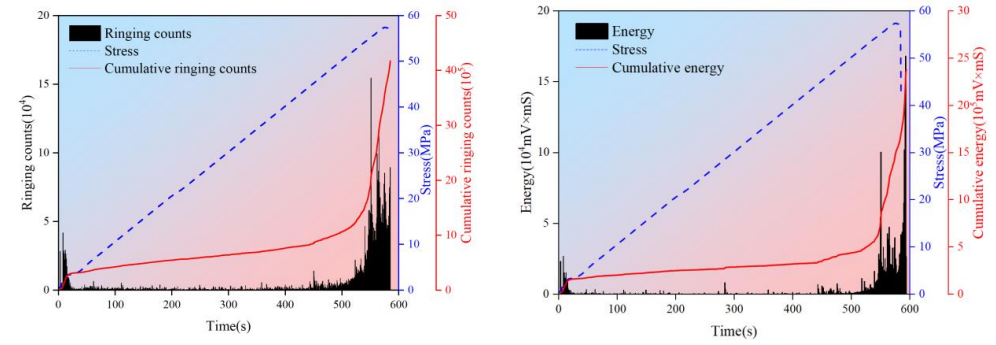

(c)0.38

Fig.5 Loading,ringing counts,energy,related to time

At the end of the OA stage (about 8-10% of the peak stress), the primary microcracks inside the concrete reach the limit of compression closure, and the microcracks start to open again, and the contact between different interfaces inside the concrete becomes less and the friction becomes smaller, so the ringing count and energy decrease at the end of the OA stage.

After entering the AB phase (about 10-70% of the peak stress), the AE ringing counts and energy remain extremely low, and the specimen enters the AE quiet period. In this phase, the nascent microcrack starts cracking from the ITZ which is the weakest in the three-phase composition, and AE signals are extremely weak. As the primary microcrack is still developing, it is still essentially an "extension" of the crack tip in a relatively weak paste, rather than a brittle "cracking". The occasional low amplitude jumps in ringing counts and energy during this period may be the result of a small number of cracks penetrating by chance. However, in general, the

internal microcracks in the AB stage were not destabilized and the concrete specimens still maintained good integrity, although they formed a certain scale.

After entering the BC stage, the AE ringing counts and energy increase sharply, but not suddenly from the critical point B to the limit value. In the early BC stage (about 70-97% of the peak stress), the violent increase of AE ringing count and energy still maintains a certain gradient, and the limit jump of AE ringing count and energy only occurs in the late BC stage.

This indicates that most of the cracks inside the concrete are not yet penetrated and destabilized in the early BC stage, and the sharp increase of AE ringing count and energy may be caused by the real "cracking" of the primary cracks and microcracks. At this point, the cracks are still in the stable expansion stage.

In the late BC stage (about 97% of the peak stress), the cracks enter the non-stable expansion stage, where the previously formed cracks of a certain size penetrate each other and destabilize rapidly. At the same stage, the development of cracks is no longer confined to the weaker paste, and some of the aggregates in the concrete also crack at this time. Therefore, this stage produces high amplitude and high frequency AE signals, and both AE ringing counts and energy take a huge jump.

3.3.Sensitivity and discreteness

Next, the relationship between the cumulative and peak counts and w/c ratio should be analyzed.

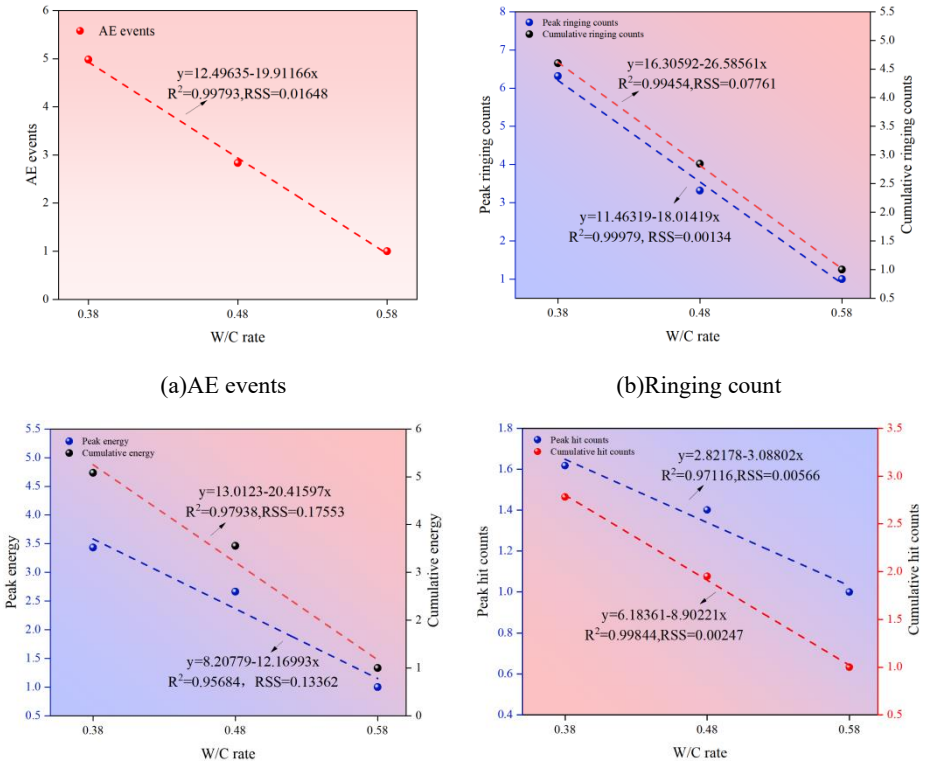

(a)AE events (b)Ringing count

(c)Energy (d)Hit count

Fig.6 Variation of AE parameters of concrete with different w/c ratios

We took a set of specimens with w/c ratio of 0.58 as a reference and normalized the parameters measured for each group of specimens, as shown in Figure 6. It can be clearly seen that the number of AE events, hit counts, CR and CE during uniaxial compression have a good

linear monotonic relationship with the w/c ratio. The sensitivity of AE parameters to w/c ratio meets the requirements of engineering accuracy.

All these parameters increased significantly with decreasing w/c ratio. The peak ringing counts and CR increased by 432 % and 460 %, respectively, the CE increased by 308 % and the peak impact count increased by 62% when the w/c ratio was reduced from 0.58 to 0.38. Residual sum of squares (RSS) was used to evaluate the discreteness of the parameters. The RSS in each group is less than 0.2, indicating that the discreteness of the parameters is small and the parameters tend to be linear.

3.4.Frequency domain analysis

The collected AE signal is transformed by FFT. According to statistics, AE signals in this paper can be divided into four types, as shown in Figure 7. The first type of signal is concentrated in the OA stage. Its main frequency is 33.20 kHz, and the dominant frequency band is 33.20 kHz~166.02 kHz. The main frequency of the second type of signal is 151.37 kHz, and the dominant frequency band is 33.20 kHz~151.37 kHz. These signals are concentrated in the early AB stage and may be related to ITZ cracking. The main frequency of the third type of signal is 153.32 kHz, and the dominant frequency band is 153.32 kHz~260.74 kHz. This type of signal widely exists in the middle and late stages of AE activity, which is very consistent with the period of stable crack growth described in section 3.1.2.The fourth type of signal appears in the late BC stage. The main frequency is 258.79 kHz, the dominant frequency band is 159.18 kHz258.79 kHz, and AE signals above 300 kHz are obviously present in the spectrum diagram of this type of signal.According to the evolution process of AE signal spectrum, the dominant frequency band of AE signal shows a trend of transferring from low frequency to high frequency during concrete loading.

Further, there is a significant correlation between AE impact count, peak frequency and damage stage, as shown in Fig.8. The hit counts of concrete with different water-cement ratios are distributed within 30~270 kHz. In the OA stage, AE hit counts are mainly distributed in 30~50 kHz and 130~170 kHz. In the AB phase, AE hit counts increases in the above two frequency bands, and also appears in 250~270kHz. In the BC stage, AE hit counts distribution range increased from the original 3 frequency bands to 5 frequency bands (30~50 kHz, 130~170 kHz, 175~185k Hz, 220~230 kHz, 250~270 kHz). This phenomenon indicates that the increase of the main frequency of acoustic emission can be regarded as the precursor information of the main crack of concrete specimens.

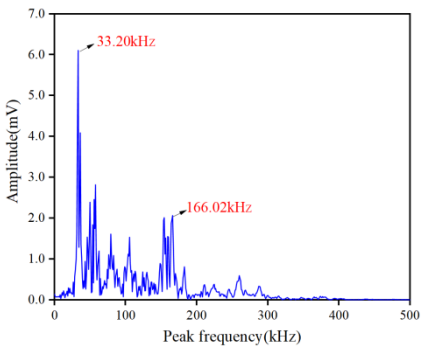

(a)OA stage signal

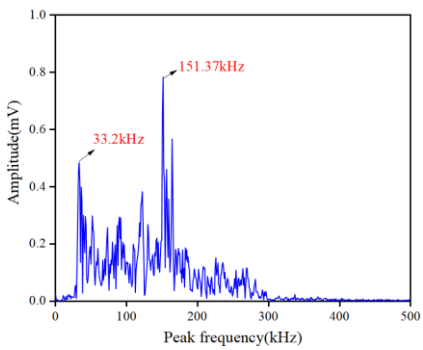

(b)AB stage signal I

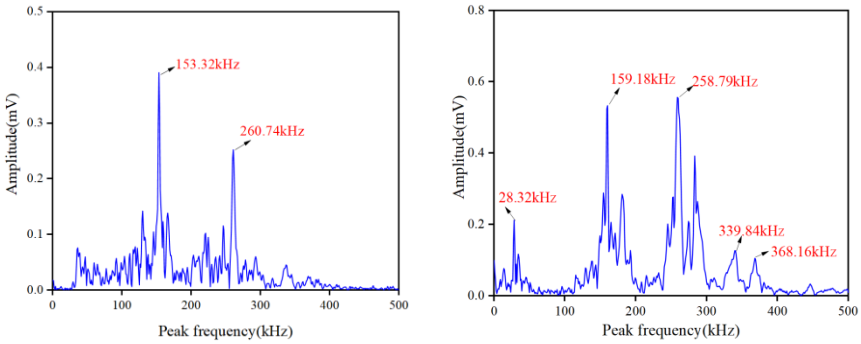

(c)AB stage signal II (d)BC stage signal

Fig.7 AE frequency diagram of concrete under uniaxial compression

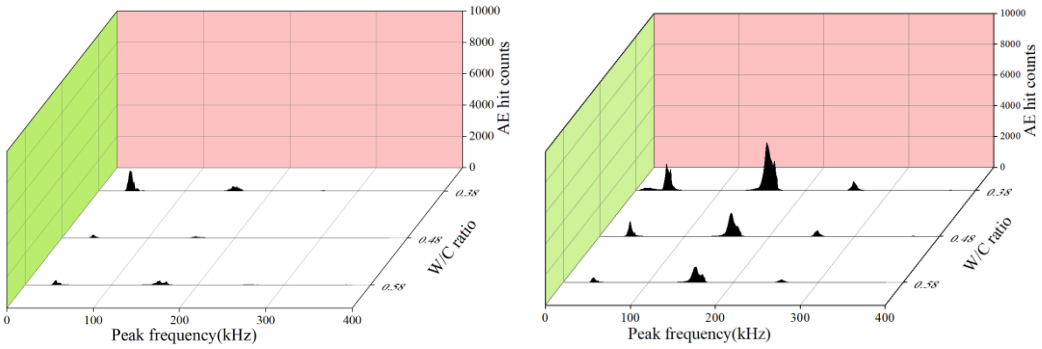

(a)OA stage (b)AB stage

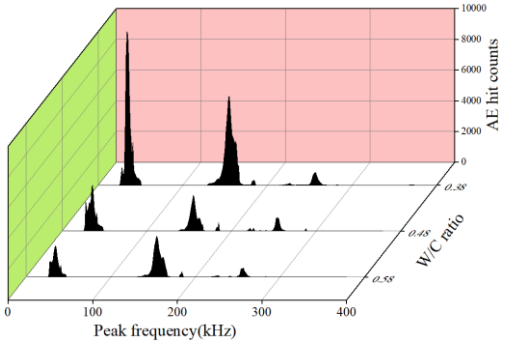

(c)BC stage

Fig.8 Peak frequency-AE hit counts distribution of concrete during uniaxial compression

4. Damage model

4.1.Damage characteristics

From the above analysis, we can see the close relationship between AE parameters and concrete damage process.We can reflect the internal deterioration process of concrete to a certain extent through the change of AE parameters. Many studies[35] have confirmed the feasibility of using AE parameters to evaluate material damage. B-value method[39] is one of the most commonly used AE damage evaluation methods at present. The change of b-value can reflect the active degree of AE activity and provide an omen for the instability of the material. However, the size of the b-value is affected by artificially set parameters such as the starting amplitude and the

amplitude interval. Therefore, b-value method has unavoidable and difficult to estimate errors. In order to avoid such errors, we try to use the characteristics of AE signal itself to evaluate the damage of concrete, so as to avoid introducing additional errors. In Section 3.2, the change of AE frequency band is proposed as the precursor of major rupture. In this section, AE parameters will be used to evaluate the whole damage process of concrete.

Tang and Xu[47] It is assumed that the concrete fine microscopic unit strength obeys Weibull distribution, which fits well with this study, so the same distribution density function is used in this paper as follows

$$F(\sigma)=\frac{m}{\sigma_0}(\frac{\sigma}{\sigma_0})^{m-1}\exp[-(\frac{\sigma}{\sigma_0})^m] \quad \text{eq.(1)}$$

where σ is the random variable of Weibull distribution,σ_0 is the scale parameter, and m is the material distribution uniformity.

The damage factor D can be expressed by Equations 2 and 3

$$\frac{dD}{d\sigma}=F(\sigma) \quad \text{eq.(2)}$$

$$D=\int_0^{\sigma}F(\sigma)d\sigma=1-\exp[-(\frac{\sigma}{\sigma_0})^m] \quad \text{eq.(3)}$$

The AE technique can measure the development state of microcracks under external load and infer the evolution process of microcracks in concrete accordingly. Combining with Figures 4-5, it can be found that the AE event counts, CR and CE are well correlated with both the compressive damage process and w/c of concrete, so the method in reference[48] is referred to below. The cumulative AE counts (event counts, CR or CE) of the whole section of the specimen at complete damage are set to C_m , and accordingly, the cumulative AE counts at stress level σ is expressed as

$$C=C_m\int_0^{\sigma}F(\sigma)d\sigma \quad \text{eq.(4)}$$

Equation 4 is compared with equation 3 to obtain the relationship between D and C

$$D=\frac{C}{C_m} \quad \text{eq.(5)}$$

Next, characterizing the damage of concrete with AE parameters can be achieved if the relationship between C and the damage process of concrete can be modeled. For this purpose, it is assumed that the relationship between C and the stress level σ is

$$C=C(\sigma) \quad \text{eq.(6)}$$

Substituting Eq. 6 into Eq. 4 and deriving the derivative for both ends

$$F(\sigma)=\frac{dC(\sigma)}{C_m d(\sigma)} \quad \text{eq.(7)}$$

Rewriting Equation 7 gives the stress level σ The relationship between damage variables and AE accumulation under stress level

$$D=\frac{1}{C_m}\int_0^{\sigma}dC(\sigma) \quad \text{eq.(8)}$$

To clarify the relationship between C and σ, the relationship between cumulative AE event counts, CR and CE and stresses during uniaxial compression of concrete with different w/c ratios were analyzed in this paper, as shown in Figure 9, respectively. Fitting the data in Fig. 6 (the results are shown in Table 4), it is found that the fitting results of AE event number are poor, while the relationships between CR and CE and σ are in good agreement with the fifth order polynomial shown in Eq. 11, and the accuracy meets the engineering requirements. This indicates that although AE event number, ringing count and energy all have a good linear relationship with w/c ratios in Figure 9, ringing count and energy are better indicators than AE event number to evaluate the concrete damage process.

$$C = a + b\sigma + c\sigma^2 + d\sigma^3 + e\sigma^4 + f\sigma^5 \qquad \text{eq.(9)}$$

Substituting equation 9 into equation 7 gives

$$F(\sigma) = \frac{b + 2c\sigma + 3d\sigma^2 + 4e\sigma^3 + 5f\sigma^4}{C_m} \qquad \text{eq.(10)}$$

Integrating Equation 10 yields a damage evaluation model based on AE accumulation

$$D = \frac{b\sigma + c\sigma^2 + d\sigma^3 + e\sigma^4 + f\sigma^5}{C_m} \qquad \text{eq.(11)}$$

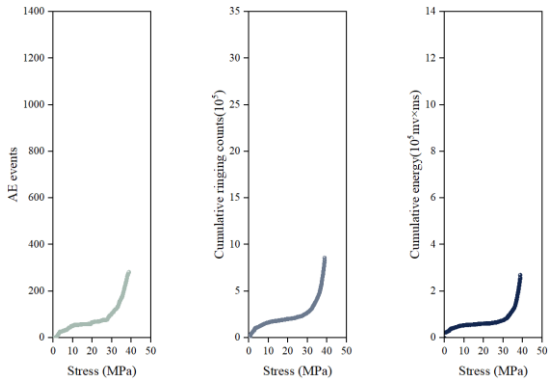

(a)0.58

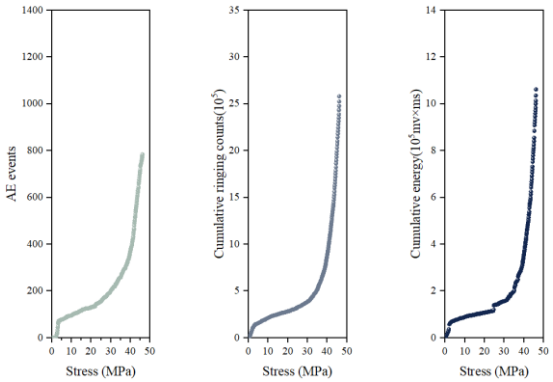

(b)0.48

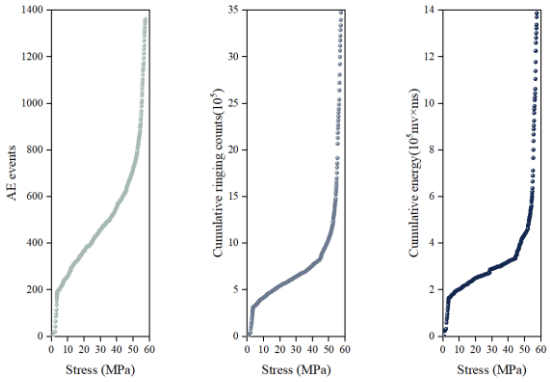

(c)0.38

Fig.9 The relationship between the cumulative value of AE parameters

Table.4 Fitting results of AE count,AE ringing count and energy

W/C ratio	AE parameter	a	b	c	d	e	f	R^2
0.58	AE events	-21.88279	14.97791	-0.92953	-0.01906	0	0	0.99035
	AE ringing counts	-21785.90503	53566.41113	-6674.61458	428.94881	-13.08131	0.15215	0.99617
	Energy	1794.28119	17412.06248	-2421.01085	162.32724	-5.03139	0.0584	0.99293
0.48	AE events	41.41146	0.94132	0.84398	-0.04766	7.91495×10^{-4}	0	0.99116
	AE ringing counts	-45682.79353	83980.21228	-10821.97884	665.8099	-18.48311	0.19136	0.99857
	Energy	-19397.84337	40727.11583	-5526.45526	335.47231	-9.05853	0.09093	0.99817
0.38	AE evens	-35.24406	72.34868	-6.37228	0.28341	-0.0057	4.2433×10^{-5}	0.99168
	AE ringing counts	-191741.54795	190523.94565	-20404.7059	978.61077	-20.65496	0.1583	0.9669
	Energy	-58087.36345	82226.20764	-8755.93217	414.74575	-8.66724	0.06585	0.95452

4.2.Discussion

To simplify the analysis process, the stress value corresponding to the peak stress is set as stress level 1, and the stress level of the stress-free state before the start of loading is set as 0. Thus, the whole loading process is divided into 10 stress levels, and the relationship between AE events, CR and CE and the stress levels of the specimen can be obtained.

As shown in Figure 10, the relationship between D and stress level can also be roughly divided into the same OA, AB, and BC stages as described previously. Among them, the two damage variables D based CR and CE have good agreement, while the damage variable D-AE

event based on the number of AE events has some dispersion from D based on the other two parameters. Therefore, we believe that CR and CE can better characterize the damage stage of concrete.

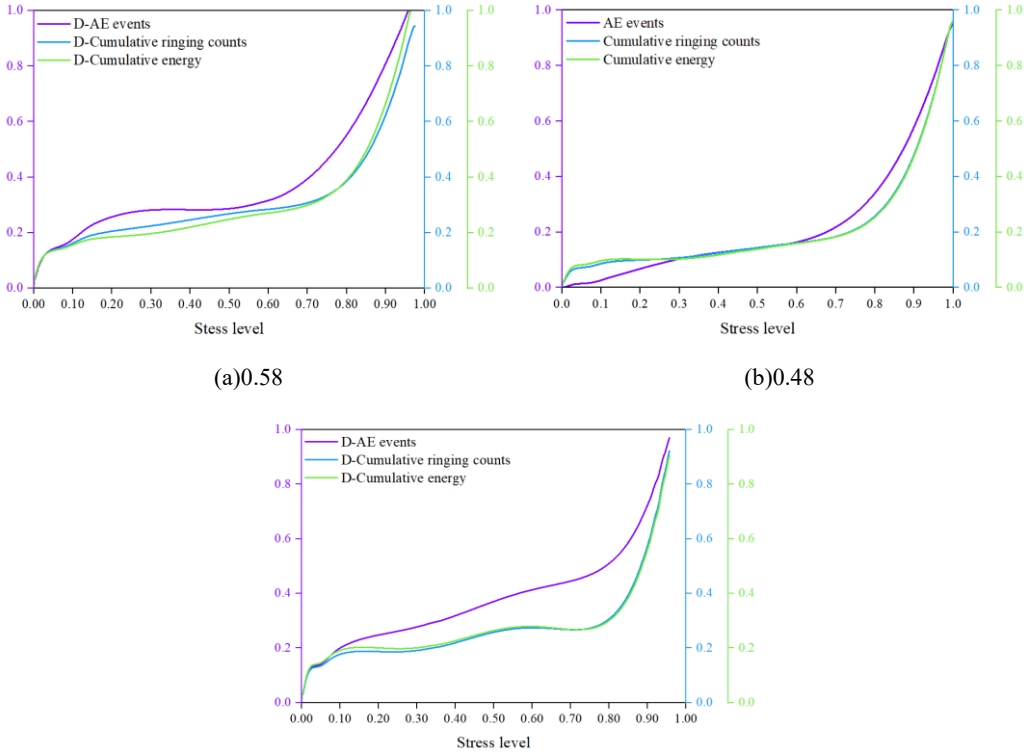

(a)0.58 (b)0.48

(c)0.38

Fig.10 The relationship between damage variable D and strain

There is a small decrease in the middle of the D-Cumulative ringing counts and D-Cumulative ringing energy curves for the 0.48 and 0.38 groups, corresponding to the occasional K curve less than 0 in the middle. This small decrease in the damage variable D does not represent a decrease in the degree of damage, but rather indicates that some degree of jump in ringing counts and energy occasionally occurs during the AB phase. This phenomenon is explained in Section 3.2 of this paper as a possible result of the occasional penetration of a small number of cracks. A small number of cracks produce an AE signal with a certain intensity at the time of penetration, after which the specimen returns to a quiet period of AE. This situation does not have much influence on the classification of the damage level.

At the end of the D curve there may be a situation where D is not equal to 1. This is because in the differentiation of Eq. 11 we eliminate the constant term a. We can observe the change in the damage phase by a simple mathematical method - by observing the change in the slope of the tangent line K of the D-CR and D-CE curves, K can be obtained from Eq. 12 is obtained.

$$K = \frac{b + 2c\sigma + 3d\sigma^2 + 4e\sigma^3 + 5f\sigma^4}{C_m} \qquad \text{eq.(12)}$$

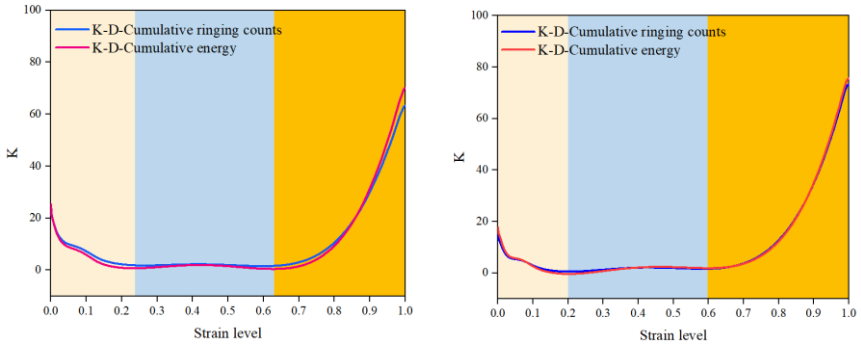

(a)0.58 (b)0.48

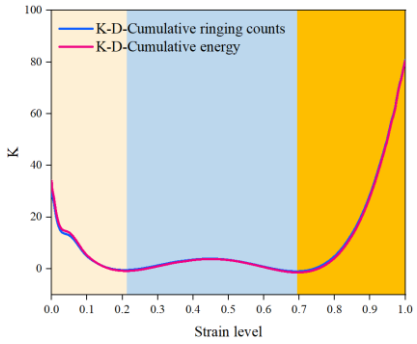

(c)0.38

Fig.11 Slope change diagram of damage variable *D*

As shown in Figure 11, the *K*-curves of D-CR and D-CE match well, and each set of curves can be divided into three stages of "falling - rising - falling" at the obvious turning points 1 and 2. In order to improve the applicability of the damage evaluation model in this paper, we should analyze the turning points of the three sets of K curves and their corresponding D values, and take the average value of D for each set as the evaluation criterion. The relevant data are shown in Table 5. The evaluation criteria of the compressive damage process are shown in Figure 12. we believe that the concrete is in a slightly damaged state in the OA stage, a moderately damaged state in the AB stage, and a heavily damaged state in the BC stage. There is an obvious turning point of the K curve between adjacent stages, which is a phenomenon worthy of attention.

Table.5 K-curve turning point

W/C ratio	Turning point 1			Turning point 2		
	Stress level	D-CR	D-CE	Stress level	D-CR	D-CE
0.58	0.238	0.211	0.188	0.631	0.286	0.273
0.48	0.200	0.100	0.102	0.598	0.161	0.159
0.38	0.213	0.186	0.200	0.695	0.270	0.272

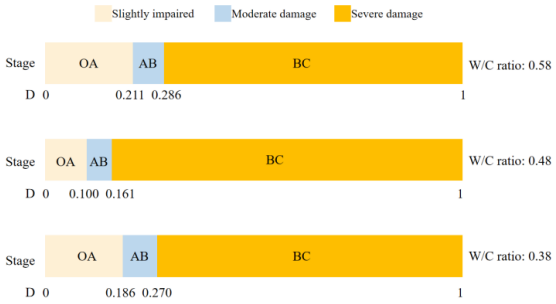

(a)D-Cumulative ringing counts

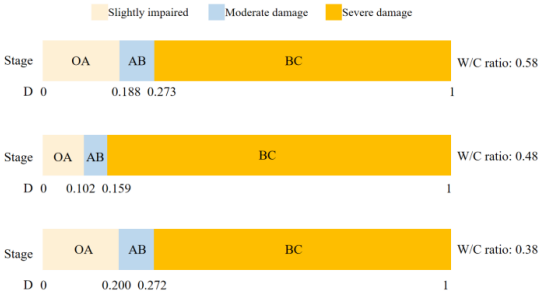

(b)D-Cumulative energy

Fig.12 Evaluation criteria for concrete under compression

4.3.Advantages and drawbacks

Damage assessment methods based on AE frequency band variation and AE characteristic parameters are presented in section 3.2 and section 4.2 respectively. Compared with the existing methods, the method proposed in this paper is based on the characteristics of AE signal itself to avoid the extra error introduced by humans. The frequency band method has the advantage of simplicity. As long as an increase in the number of high frequency bands is detected, an early warning can be given for concrete cracking. The parameter model can monitor the whole process of concrete damage, which is more precise than the frequency band method.

Unfortunately, the quantitative relationship between the damage evaluation model established in this paper and the water-cement ratio is not clear. This is affected by the randomness of the sample. It is worth considering how to further clarify the quantitative relationship between water-cement ratio and *D*.

5. Conclusion

The main findings are as follows:

1. Using AE characteristic parameters, the failure process of concrete specimens can be divided into three stages: the initial stage (OA), the stable stage(AB) and the active stage (BC). There is a good correspondence between the variation trend of AE characteristic parameters and the development of micro-cracks, which indicates that monitoring the failure process of concrete by AE technology is helpful to understand the failure mechanism of concrete and evaluate the damage degree of concrete.

2. With the development of concrete damage process, the dominant frequency band of AE signal presents a trend of deviation from low frequency to high frequency. The dominant

frequency band in the initial stage is 33 kHz~170 kHz; In the stable phase, the dominant frequency band shifts from 33 kHz~150 kHz to 153 kHz~260 kHz. The dominant frequency band in the active phase is 159.18 kHz~258.79 kHz.

3. There is a significant correlation between AE impact count, peak frequency and damage stage. The distribution frequency of AE impact counts showed an increasing trend. The OA phase has 2 bands, the AB phase has 3 bands, and the BC phase has 5 bands. The phenomenon of increasing frequency band can be regarded as the precursor of main fracture of concrete specimen.

4. The concrete damage evaluation model D established in this paper based on AE cumulative ringing count and total energy is very consistent with the main stages of the concrete failure process, and its slope change curve K has significant changes in different damage stages, so it is feasible to use this model as the evaluation standard of compressive damage of concrete materials in engineering.

This paper is a preliminary exploration of the relationship between concrete components and AE response, and the following aspects need to be studied in the future.

1. The next step is to consider the effects of loading rate and aggregate particle size on AE response and the AE characteristics of concrete under different working conditions (e.g., different ages, temperatures, moisture contents, loading methods, etc.).

2. It is worth studying in the future to consider the effect of ITZ and the porosity on crack development and the AE characteristics during the crack development by numerical simulation method.

3. The object of this paper is to study plain concrete specimens with different w/c ratios, and the main consideration is the effect of internal pores and microcracks on the response of AE parameters in plain concrete specimens under uniaxial compression. The attenuation law[49] and stress dependence[50] of AE waves in concrete with different w/c ratios need to be further investigated.

4. Reinforcement may lead to the changes in AE characteristics of concrete. Therefore, the future research will be investigation the propagation characteristics of AE waves in reinforced concrete structures, the attenuation law and the AE response during damage, so as to achieve the damage assessment and defect localization accuracy of reinforced concrete structures.

5. Using the digital image correlation (DIC) technique as the "eye" to monitor the structural deformation, and the AE technique as the "ear" to monitor the structural damage signal. It may be a possible breakthrough direction which combines these two methods[51] .

Acknowledgments

The first author would like to acknowledge the financial support provided by the National Natural Science Foundation of China (Grant No. 51968014) , Guangxi Natural Science Foundation (Grant No. 2022GXNSFAA035553), Key R&D projects in the Guangxi Autonomous Region (Grant No. AA20302006) and Innovation Project of Guangxi Graduate Education (Grant No. YCSW2023367).

References

[1] Grosse C U, Ohtsu M, Aggelis D G, et al. AE Testing: Basics for Research – Applications in Engineering. Cham: Springer International Publishing. 2022.

[2] Nilsen A U, Monteiro P J. Concrete:a three phase material. Cem Concr Res. 1993;23,147–151.
[3] Holford K M, Carter D C. AE source location. Key Eng Mater. 1999;162–171.
[4] Liu G, Wang S, Xie Y, et al. Damage detection of offshore platforms using AE analysis. Rev Sci Instrum. 2018;89:115005.
[5] Xu Y, Chen S. A method for modeling the damage behavior of concrete with a three-phase mesostructure. Constr Build Mater. 2016;102:26-38.
[6] Wu K, Chen B, Yao W. Study of the influence of aggregate size distribution on mechanical properties of concrete by acoustic emission technique. Cem Concr Res. 2001;31:919-923.
[7] Chen B, Liu J. Investigation of effects of aggregate size on the fracture behavior of high performance concrete by AE. Constr Build Mater. 2007;21:1696-1701.
[8] Elaqra H, Godin N, Peix G, et al. Damage evolution analysis in mortar, during compressive loading using AE and X-ray tomography: Effects of the sand/cement ratio. Cem Concr Res. 2007;37:703-713.
[9] Lee J, Kim H, Oh T. Acoustic Emission Characteristics during Uniaxial Compressive Loading for Concrete Specimens according to Sand Content Ratio. KSCE J Civ Eng. 2020;24:2808-2823.
[10] Wang Y, Chen S J, Zhao H T, et al. Acoustic emission characteristics of interface between aggregate and mortar under shear loading. Russ J Nondestr Testi. 2015;51:497-508.
[11] Wang Y. et al. Experimental study of effects of water-cement ratio on the AE rate “a” values in concrete. Russ J Nondestruct Test. 2017;53:620–635.
[12] Ranjith P G, Jasinge D, Song J, et al. A study of the effect of displacement rate and moisture content on the mechanical properties of concrete: Use of AE. Mech. Mater. 2008;40: 453-469.
[13] Kocur G K, Saenger E H, Vogel T. Elastic wave propagation in a segmented X-ray computed tomography model of a concrete specimen. Constr Build Mater, 2010:2393–2400.
[14] Kocur G K, Vogel T, Saenger E H. Crack localization in a double-punched concrete cuboid with time reverse modeling of acoustic emissions. Int J Fract. 2011;171:1-10.
[15] Li G, Zhang L, Zhao F, et al. Acoustic Emission Characteristics and Damage Mechanisms Investigation of Basalt Fiber Concrete with Recycled Aggregate. Materials. 2020;13:4009.
[16] Fu L, Jiao Y, Chen X, et al. Evaluation Approach of Fracture Behavior for Asphalt Concrete with Different Aggregate Gradations and Testing Temperatures Using Acoustic Emission Monitoring. Materials. 2021;14:4390.
[17] Gollob S, Kocur G K. Analysis of the wave propagation paths in numerical reinforced concrete models. J Soune Vib. 2021;494:115861.
[18] Chen X, Wu S. Influence of water-to-cement ratio and curing period on pore structure of cement mortar. Constr Build Mater. 2013;38:804-812.
[19] Winslow D, Liu D. The pore structure of paste in concrete. Cem Concr Res. 1990;20:227-235.
[20] Farnam Y, Geiker M R, Bentz D, et al. AE waveform characterization of crack origin and mode in fractured and ASR damaged concrete. Cem Concr Compos. 2015;60:135-145.
[21] Zhang S, Zhang C, Liao L, et al. Numerical study of the effect of ITZ on the failure behaviour of concrete by using particle element modelling[J]. Constr Build Mater. 2018;170:776-789.
[22] Chen H, Xu B, Mo Y L, et al. Behavior of meso-scale heterogeneous concrete under uniaxial

tensile and compressive loadings. Constr Build Mater, 2018;178:418-431.
[23] Peng Y, Wang Q, Ying L, et al. Numerical Simulation of Dynamic Mechanical Properties of Concrete under Uniaxial Compression. Materials, 2019;12:643.
[24] Torrence C, Trageser J, Jones R, et al. Sensitivity of the strength and toughness of concrete to the properties of the interfacial transition zone. Constr Build Mater. 2022;336:126875.
[25] Akçaoğlu T, Tokyay M, Çelik T. Effect of coarse aggregate size and matrix quality on ITZ and failure behavior of concrete under uniaxial compression. Cem Concr Compos. 2004;26:633-638.
[26] Huang Y, He X, Wang Q, et al. Deformation field and crack analyses of concrete using digital image correlation method. Front Struct Civ Eng. 2019;13:1183-1199.
[27] Kim Y, Lee K, Bang J, et al. Effect of W/C Ratio on Durability and Porosity in Cement Mortar with Constant Cement Amount. Adv Mater Sci Eng. 2014;2014:1-11.
[28] Peng Y, Su L, Wang Y, et al. Analysis of the Effect of Porosity in Concrete under Compression Based on DIP Technology. J Mater Civ Eng. 2022;34:04021376.
[29] Zhou Y, Yu X, Guo Z, et al. On AE characteristics, initiation crack intensity, and damage evolution of cement-paste backfill under uniaxial compression. Constr Build Mater. 2021;269:121261.
[30] Li D, Wang E, Kong X, et al. Mechanical behaviors and AE fractal characteristics of coal specimens with a pre-existing flaw of various inclinations under uniaxial compression. Int J Rock Mech Min. 2019;116:38-51.
[31] Su G, Gan W, Zhai S, et al. AE precursors of static and dynamic instability for coarse-grained hard rock. J Cent South Univ. 2020,27:2883-2898.
[32] Du K, Li X, Tao M, et al. Experimental study on acoustic emission (AE) characteristics and crack classification during rock fracture in several basic lab tests. Int J Rock Mech Min. 2020;133:104411.
[33] Xue G, Yilmaz E. Strength, acoustic, and fractal behavior of fiber reinforced cemented tailings backfill subjected to triaxial compression loads. Constr Build Mater. 2022;338:127667.
[34] Li X, Chen S, Liu S, et al. AE waveform characteristics of rock mass under uniaxial loading based on Hilbert-Huang transform. J Cent South Univ. 2021;28:1843-1856.
[35] Zhou M, Liao J, An L, et al. Analysis of stress-induced cracks in concrete and mortar under cyclic uniaxial compression. Constr Build Mater. 2018;187:652-664.
[36] Xargay H, Ripani M, Folino P, et al. AE and damage evolution in steel fiber-reinforced concrete beams under cyclic loading. Constr Build Mater. 2021;274:121831.
[37] Wu Y, Li S, Wang D. Characteristic analysis of AE signals of masonry specimens under uniaxial compression test. Constr Build Mater. 2019;196:637-648.
[38] Xu J, Niu X, Ma Q, et al. Mechanical properties and damage analysis of rubber cement mortar mixed with ceramic waste aggregate based on AE monitoring technology. Constr Build Mater. 2021;309:125084.
[39] Dong L, Zhang L, Liu H, et al. Acoustic Emission b Value Characteristics of Granite under True Triaxial Stress. Mathematics. 2022;10:451.
[40] Wang Y, He M, Ren F, et al. Source analysis of acoustic emissions during granite strain burst. Geomatics Nat Hazards Risk. 2019;10:1542-1562.
[41] Shah S, Chandra K. Use of acoustic emissions in flexural fatigue crack growth studies on

concrete. Eng Fract Mech. 2012;87:36-47.
[42] Ju Y, Wu X. Acoustic Emission Characteristics and Failure Prediction of the Granite with Orthogonal Cracks under Compressive Loading. Adv Civ Eng. 2020;2020:1-10.
[43] Yu Y, Zhao D, Fegn G, et al. Energy Evolution and Acoustic Emission Characteristics of Uniaxial Compression Failure of Anchored Layered Sandston. Front Earth Sci. 2022;10:841598.
[44] Lei X, Li S, Liu L. Seismic b-Value for Foreshock AE Events Preceding Repeated Stick-Slips of Pre-Cut Faults in Granite. Appl Sci. 2018;8:2361.
[45] Burud N, Chandra K. Application of generalized logistic equation for b-value analysis in fracture of plain concrete beams under flexure. Eng Fract Mech. 2019;210:228-246.
[46] Iturrioz I, Lacidogna G, Carpinteri A. Acoustic emission detection in concrete specimens: Experimental analysis and lattice model simulations. Int J Damage Mech. 2014;23: 327-358.
[47] Tang C, Xu X. Evolution and propagation of material defects and Kaiser effect function. J Seismol Res. 1990;13:203–213.
[48] Geng J, Sun Q, Zhang Y, et al. Studying the dynamic damage failure of concrete based on acoustic emission. Constr Build Mater. 2017;149:9-16.
[49] Li D, Yang K, He Z, et al. Acoustic emission wave velocity attenuation of concrete and its application in crack localization. Sustainability. 2020;12:7405.
[50] Li G, Gu J, Ren Z, et al. Damage Evaluation of Concrete under Uniaxial Compression Based on the Stress Dependence of AE Elastic Wave Velocity Combined with DIC Technology. Materials. 2021;14:6161.
[51] Verbruggen S, De Sutter S, Iliopoulos S, et al. Experimental structural analysis of hybrid composite-concrete beams by digital image correlation (DIC) and acoustic emission (AE). J Nondestruct Eval. 2016;35:2.
[52] Dai S, Liu X, Nawnit K. Experimental Study on the Fracture Process Zone Characteristics in Concrete Utilizing DIC and AE Methods. Appl Sci. 2019;9:1346.
[53] Liu S, Ma H. Estimation of the stress level on a cross section of a reinforced concrete beam via AE Intensity Distribution (AID) analysis. Constr Build Mater. 2018;164:463-476.
[54] Lacidogna G, Piana G, Accornero F, et al. Multi-technique damage monitoring of concrete beams: AE, digital image correlation, dynamic identification. Constr Build Mater. 202;242:118114.
[55] Boniface A, Saliba J, Sbartaï Z, et al. Evaluation of the AE 3D localisation accuracy for the mechanical damage monitoring in concrete. Eng Fract Mech. 2020;223:106742.
[56] Sharma G, Sharma S, Sharma S, Fracture monitoring of steel and GFRP reinforced concrete beams using AE and digital image correlation techniques. Struct Concr. 2021;22:1962-1976.